The mechanism of hydrogen plasma passivation for poly-crystalline silicon thin film*

Li Juan(李 娟)[a)†], Luo Chong(罗 翀)[a)], Meng Zhi-Guo(孟志国)[a)],
Xiong Shao-Zhen(熊绍珍)[a)], and Hoi Sing Kwok(郭海威))[b)]

[a)] *Institute of Photo-Electronics, Tianjin Key Laboratory for Photo-Electronic Thin Film Devices and Technology, Nankai University, Tianjin* 300071, *China*

[b)] *Department of Electronic and Computer Engineering, The Hong Kong University of Science and Technology, Clear Water Bay, Kowloon, Hong Kong, China*

(Received 10 December 2012; revised manuscript received 14 April 2013)

The mechanism of hydrogen plasma passivation for poly-crystalline silicon (poly-Si) thin films is investigated by optical emission spectroscopy (OES) combined with Hall mobility, Raman spectra, absorption coefficient spectra, and so on. It is found that different kinds of hydrogen plasma radicals are responsible for passivating different defects in poly-Si. The H_α with lower energy is mainly responsible for passivating the solid phase crystallization (SPC) poly-Si whose crystallization precursor is deposited by plasma-enhanced chemical vapor deposition (PECVD). The H^* with higher energy may passivate the defects related to teh Ni impurity around the grain boundaries more effectively. In addition, H_β and H_γ with the highest energy are required to passivate intra-grain defects in the poly-Si crystallized by SPC but whose precursor is deposited by low pressure chemical vapor deposition (LPCVD).

Keywords: hydrogen plasma, passivation, poly-Si, mechanism

PACS: 51.50.+v, 52.25.–b, 61.82.Fk **DOI:** 10.1088/1674-1056/22/10/105101

1. Introduction

Poly-crystalline silicon (poly-Si) thin films prepared on glass substrate at temperature lower than 600 °C is a promising technology to make large area electronic devices, owing to its advantages of lower cost than mono-crystalline silicon, and higher mobility and greater stability than amorphous silicon. It dramatically attracts scientific interest because of the possible application in flat panel displays[1] and solar cells.[2] However, poly-Si thin films have many more defects in grain boundaries[3] or intra-grains,[4] which severely affect the performances and stabilities of the devices made of such a poly-Si material. The hydrogen plasma treatment is one of the most effective methods to passivate the defects in poly-Si materials and devices.[5,6] Generally, hydrogen in silicon thin film can be attracted not only to any strained regions of the crystal but also to self-traps.[7,8] On the one hand, hydrogen can attach itself to the dangling bonds and neutralize them, thus reducing the number of recombination centers.[9] However, on the other hand, hydrogen plasma can etch Si atoms and bombard the surface of poly-Si, inducing some new defects during passivation.[10] Therefore, to improve the poly-Si performance more effectively, an investigation of its passivation mechanism is necessary. In this work, the physical mechanism of the hydrogen passivation is investigated deeply with different kinds of poly-Si: MIC (metal-induced crystallization) poly-Si and solid phase crystallization (SPC) poly-Si. Moreover, different amorphous silicon thin films are used as the crystallization precursors. The *in-situ* optical emission spectroscopy (OES) is adopted during passivation, meanwhile, the corresponding properties of the passivated poly-Si thin films are characterized.

2. Experiments

The 100-nm thick a-Si thin films were deposited by LPCVD (low pressure chemical vapor deposition) and PECVD (plasma-enhanced chemical vapor deposition) respectively on Eagle 2000 Corning glass followed by crystallization with SPC or the MIC method. The PECVD a-Si was deposited with hydrogen diluted silane (SiH_4:H_2=1:4) at a flow rate of 40 sccm. The growth rate was 50 Å/min under a total gas pressure of 43 Pa. The substrate temperature and the radio frequency (RF) active power is of 270 °C and of 10 W respectively. Dehydrogenation was performed before the crystallization process. The LPCVD a-Si was deposited with SiH_4 at 600 mTorr (1 Torr = 1.33322×10^2 Pa) and 550 °C, and the growth rate was 20 Å/min–25 Å/min. The SPC process was carried out in N_2 atmosphere for 24 h at 600 °C. The MIC process began with the deposition of Ni for 9 min by sputtering with an RF power of 7 W, followed by heating at 590 °C in N_2 atmosphere for 6 h and finally etching Ni residue on the surface of the sample. The sample using the PECVD a-Si as a precursor and crystallized by SPC is named PE-SPC,

*Project supported by the National Natural Science Foundation of China (Grant No. 61076006) and the Flat-Panel Display Special Project of China's 863 Plan (Grant No. 2008AA03A335).

†Corresponding author. E-mail: lj1018@nankai.edu.cn

© 2013 Chinese Physical Society and IOP Publishing Ltd

that using LPCVD a-Si as a precursor and crystallized by SPC is named LP-SPC, and that by crystallized MIC is named LP-MIC. The power source for hydrogen plasma treatment was an RF power device. The distance between the heater and the RF electrode was 33 mm. The hydrogen plasma passivation was under an H_2 flow rate of 30 sccm, reaction pressure of 106 Pa, an RF active power of 40 W, and a substrate temperature of 350 °C. The OES signals of the plasma were recorded by using a PR650 spectrophotometer and focalized at a position of 2 mm above the sample surface. The passivated poly-Si samples were characterized by their Hall mobility and the Raman spectra. The Raman TO peak at 520 cm^{-1} taken on single crystal was used as a reference for all our measurements. In addition, the absorption coefficients were measured by reflection and transmission spectra.

3. Results and discussion

Figure1 shows the OES result of hydrogen plasma measured after 15 min of glow discharging for different samples. No sample in the chamber is called "no sample". The OES peaks indicate the emissions contributed by different hydrogen radicals: H_α (656 nm, corresponding to $n = 3$ excited state of H), H^* (602 nm, excited state of H_2), H_β (486 nm, corresponding to $n = 4$ excited state of H), and H_γ (434 nm, $n = 5$ excited state of H). It is very clear that the H_α signals are the same for the three cases; H^* signals are the same for the cases of LP-SPC and "no-sample" but different from that in the case of LP-MIC. H_β and H_γ signals are the same for the cases of LP-MIC and "no-sample" but different from that in the case of LP-SPC. This is a very interesting phenomenon which illustrates the different passivation effects of different H plasma radicals. The peak intensities of these four kinds of hydrogen radicals against treatment time are shown in Fig. 2. As for PE-SPC, H_α consummates dominantly at the beginning of passivation treatment, and then, starts to increase at the treatment time of around 5 min. Figure 2(b) clearly shows that the changes of H_β and H_γ are much greater than those of H_α and H^*, which implies that the H_β and H_γ have significant effects on the defect passivation for LP-SPC poly-Si samples. We can observe that at the beginning of 20 min of the passivation treatment, the peak intensities of H_β and H_γ decrease obviously, and then increase. The decreases of peak intensities of H_β and H_γ should be caused by consuming the defect passivation of poly-Si. After about 45 min of H plasma treatment, only small amount of H_β and H_γ is consumed and becomes stable, which means the production and the consumption of these kinds of H radicals achieve a certain dynamic balance in chamber. For the LP-MIC sample, the H^* is mainly consumed at the beginning of 10 min during the passivation treatment.

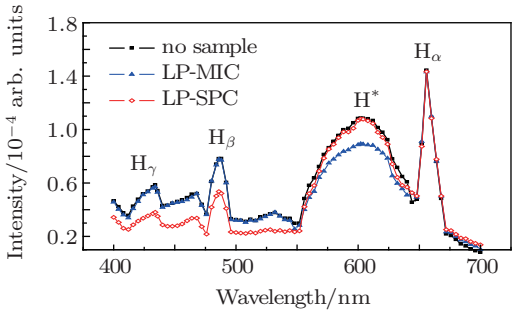


Fig. 1. (color online) Comparison of the hydrogen plasma optical emitting signals among the samples LP-SPC, LP-MIC, and no sample in chamber.

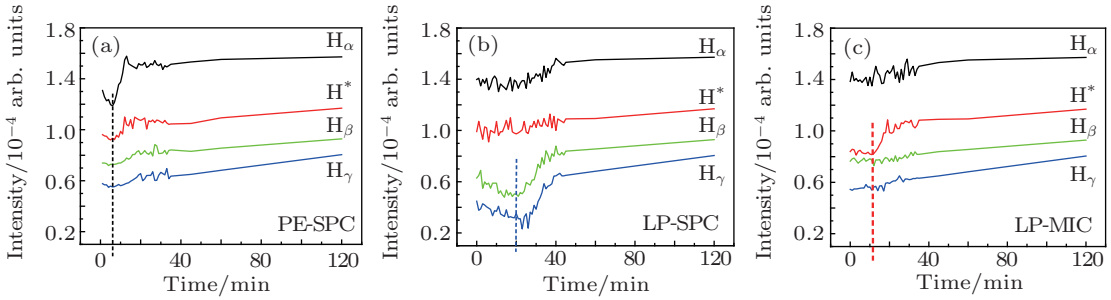


Fig. 2. (color online) Intensities of four kinds of hydrogen radicals versus H plasma treatment time with the sample of PE-SPC (a), LP-SPC (b), and LP-MIC (c).

The performances of the poly-Si samples are characterized by their Hall mobility as shown in Fig. 3. The improvement of Hall mobility is indicated by the ratio of the increased Hall mobility after the passivation treatment to the Hall mobility before the passivation treatment, which is called "gain" here. As shown in Fig. 3, for LP-SPC, after 20-min hydrogen plasma treatment, the Hall mobility is increased by over 20%. However, the longer treatment time did not lead to better performance, instead, the Hall mobility decreases. Combining the above OES results, we infer that during the first 20 min of hydrogen plasma treatment, H_β and H_γ are consummated to passivate the LP-SPC poly-Si, res1ulting in the increase of its Hall mobility. During this period, most defects in the poly-Si are passivated. Nevertheless, if the poly-Si continues to be exposed to the plasma, the bombardment effect and etching effect become critical, which create new defects[10] and degenerate the poly-Si performance. Similarly, considering Figs. 2(b), 2(c), and Fig. 3 comprehensively, we can deduce

that PE-SPC poly-Si and LP-MIC poly-Si are mainly passivated by H_α within 5 min and by H^* within 10 min respectively. The results of OES and Hall mobility measurement are matched very well, which proves the rationality of our analysis.

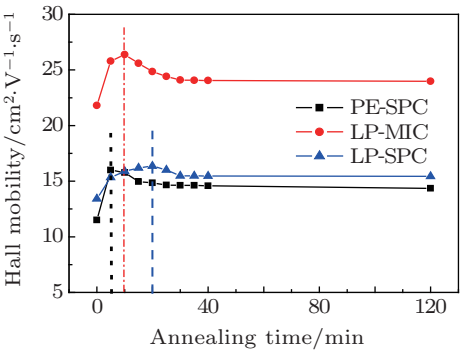


Fig. 3. (color online) Hall mobilities of poly-Si after different treatment time.

The absorption coefficient spectrum within the range of sub-band gap is adopted to analyze the passivation mechanism more deeply.

As shown in Fig. 4, the sub-band gap absorption coefficients of these three types of poly-Si samples after passivation treatment are one order of magnitude lower than before passivation, which indicates that their defect densities decrease dramatically by hydrogen plasma treatment.[11] Additionally, the sub-band gap absorption coefficient of the PE-SPC poly-Si sample is higher and improves more than that of LP-SPC or LP-MIC poly-Si sample, which illustrates that the defect density in PE-SPC poly-Si sample is larger than that in LP-SPC or LP-MIC before passivation treatment. This could possibly explain why the Hall mobility of the PE-SPC poly-Si sample is improved more than those of the other two types of poly-Si samples after hydrogen plasma passivation.

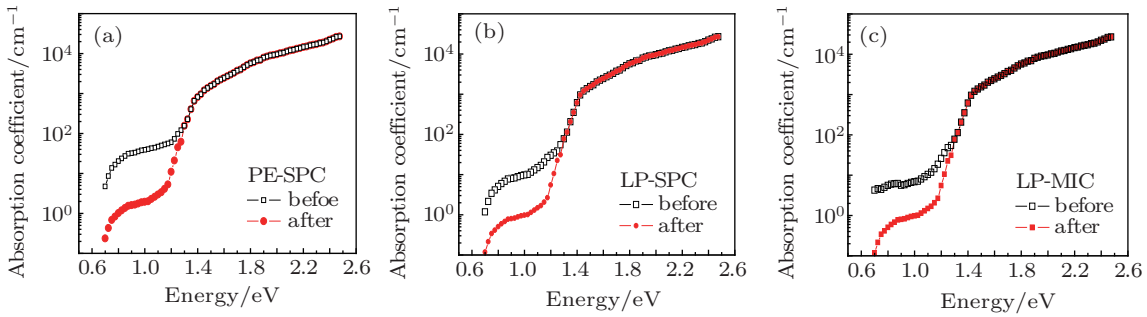


Fig. 4. (color online) Comparisons of the absorption coefficient spectrum before and after passivating the samples of PE-SPC (a), LP-SPC (b), LP-MIC (c).

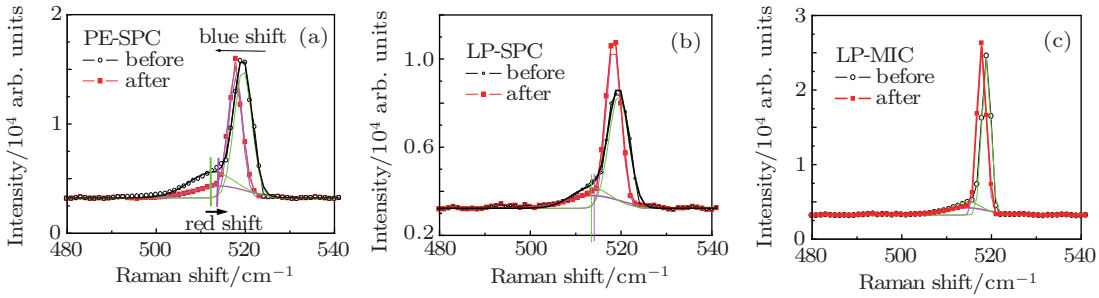


Fig. 5. (color online) Comparisons of the Raman spectra of some poly-Si samples before and after hydrogen plasma treatment.

The Raman spectrum is an important measurement to characterize the quality of a poly-Si material. The Raman spectra of the poly-Si before and after H-plasma treatment are compared in Fig. 5. As can be observed, the peaks related to TO mode in all Raman spectra each have a "blue shift" (shift to short wave number), which indicates that the tensile stress has been generated during H-plasma treatment. The stress value ε can be determined from Raman spectra from the following formulas: [12]

$$\varepsilon = -250\ (\text{MPa/cm}) \times \Delta\omega, \tag{1}$$

$$\Delta\omega = X_{\text{cp}} - X_{\text{cm}}, \tag{2}$$

where $\Delta\omega$ is the difference between the extracted poly-Si fitting peak (X_{cp}) and the single crystal silicon fitting peak (X_{cm}). In addition, we also calculate the crystal volume fraction (P_{c}) as the ratio of the integrated intensity of the 520 cm^{-1} band to the sum of the integrated intensities of $\sim$ 510 cm^{-1} and 520 cm^{-1} bands, which correspond to the crystalline phase

and the grain boundary defect, respectively, as shown as the following formula:[12]

$$P_c = I_c/(I_c + I_m). \quad (3)$$

All results are shown in Table 1. As can be observed, the $\Delta\omega$ becomes larger after H passivation treatment. We suggest that the increase of the compressive stress may be due to the fact that the lattice constant of hydrogen atom is smaller than that of silicon. Moreover, with the H-plasma treatment, the full width at half maximum (FWHM) values of the TO mode at 520 cm^{-1} of all three poly-Si samples become narrower and the P_c values become higher, illustrating the improvement of the poly-Si quality.

Table 1. Values of extracted $\Delta\omega$, FWHM, and P_c from Raman spectra.

	PE-SPC		LP-SPC		LP-MIC	
	Before treatment	After treatment	Before treatment	After treatment	Before treatment	After treatment
$\Delta\omega$	0.6	2.2	0.6	1.7	0.8	2.2
FWHM	5.1	3.6	6.1	4.3	2.5	2.3
P_c	65.10%	72.50%	73.50%	77.80%	78.60%	82.60%
ΔP_c	7.4%		4.3%		4%	

The table also shows that the P_c value of PE-SPC poly-Si is lower than those of LP-SPC and LP-MIC before H plasma passivation. This is because of its large number of dangling bond defects in the grain boundaries, which have resulted from the dehydrogenation process of the PECVD-a-Si precursor before SPC crystallization.[13] This can be indicated by the fitting peak signal around 510 cm^{-1} of the Raman spectrum of PE-SPC poly-Si in Fig. 5. Additionally, the FWHM reveals the intra-grain quality of poly-Si.[14] The FWHM of LP-SPC poly-Si is wider than those of PE-SPC and LP-MIC poly-Si before H-plasma passivation, which suggests that LP-SPC poly-Si has more intra-grain defects than the other two kinds of poly-Si materials.[14] The large decrease of the FWHM of LP-SPC poly-Si illustrates that the hydrogen radicals H_β and H_γ mainly passivate intra-grain defects. As for LP-MIC poly-Si, because of its higher crystalline quality (usually larger grain size[15]), the improvements of its P_c and FWHM by hydrogen passivation are smaller than those for the other two kinds of poly-Si materials.

From the above results of OES, absorption coefficient spectra, Raman spectra, and Hall mobility, it can be inferred that the major defects in PE-SPC poly-Si are the dangling bond defects at grain boundaries. As a kind of low energy plasma radical, H_α can effectively passivate those defects, leading to the formation of a Si–H bond with low bond energy as shown as follows:[10,17]

$$\equiv Si - + H = \equiv Si - H. \quad (4)$$

As major defects in LP-SPC poly-Si are intra-grain defects, higher energy radicals H_β and H_γ are needed to penetrate into the grains, and even to break Si–Si weak bonds firstly, and then to perform the passivation and form Si–Si strong bonds as shown in the following equation:[10,17]

$$2H + (Si - Si)_{weak} = (Si - Si)_{strong} + H_2. \quad (5)$$

But LP-MIC contains many defects related to Ni impurity whose bond energy might be greater than that of a dangling bond and lower than that of a Si–Si weak bond, so H^* radicals with middle energy are suitable to passivating this kind of defect.[10,16,17]

Some conclusions can be drawn as follows: there are four kinds of hydrogen plasma radicals in the hydrogen passivation process for poly-Si materials. It has been found that the hydrogen plasma passivation mechanism is related to the poly-Si crystallization method and the a-Si crystallization precursor. The results of OES, absorption coefficient spectra, Raman spectra, and Hall mobility indicate that the roles of the hydrogen plasma radicals depend on the defect type in the poly-Si material. Different hydrogen plasma radicals have different passivation effects. For PE-SPC poly-Si, in which the major defects are the dangling bonds at grain boundaries, low energy radicals H_α can passivate them effectively. For LP-SPC poly-Si material, in which the major defects are intra-grain defects, higher energy radicals H_β and H_γ are needed to perform the passivation effectively. For LP-MIC poly-Si, which contains many defects relative to Ni impurity, H^* radicals with middle energy are suitable to passivating this kind of defect. These results and analyses are very useful to optimize the H plasma passivation condition and make the passivation more effective.

Acknowledgment

We greatly appreciate Prof. Helmut Fritzsche for his revision of this paper.

References

[1] Gang L and Stephen J F 1993 *Appl. Phys. Lett.* **62** 2554

[2] Oliver N, Tom P, Linda M K, Alistair B S and Stuart R W 1998 *Appl. Phys. Lett.* **73** 3214

[3] Meng Z G, Li Y, Wu C Y, Zhao S Y, Li J, Man W, Kwok H S and Xiong S Z 2008 *Chin. Phys. B* **22** 046101

[4] Wu C Y, Li X D, Zhao S Y, Li J, Meng Z G and Xiong S Z 2009 *Chin. Phys. B* **18** 1237

[5] Benton J L, Doherty C J, Ferris S D, Flamm D L, Kimerling L C and Leamy H J 1980 *Appl. Phys. Lett.* **36** 670

[6] Ostapenko S, Jastrzebski L, Lagowski J and Smeltzer R K 1996 *Appl. Phys. Lett.* **68** 2873

[7] Cielaszyk E S, Kirmse K H R, Stewart R A and Wendt A E 1995 *Appl. Phys. Lett.* **67** 3099

[8] Estreicher S K 1995 *Mater. Sci. Eng.* **R14** 319

[9] Nickel N H, Johnson N M and Jackson W B 1993 *Appl. Phys. Lett.* **62** 3285

[10] Darwichea S, Nikravecha M, Morvan D, Amourouxa J and Ballutaud D 2007 *Solar Energy Materials & Solar Cells* **91** 195

[11] Warren B J, Johnson N M and Biegelsen D K 1983 *Appl. Phys. Lett.* **43** 195

[12] Kamiya T, Kishi M, Ushirokawa A and Katoda T 1981 *Appl. Phys. Lett.* **38** 377

[13] Pankove J I, Lampert M A and Tarng M L 1978 *Appl. Phys. Lett.* **32** 439

[14] Dubé C and Hanoka J I 1984 *Appl. Phys. Lett.* **45** 1135

[15] Soo Y Y, Jae Y O, Chae O K and Jang J 1998 *J. Appl. Phys.* **84** 6463

[16] Cielaszyk E S, Kirmse K H R, Stewart A and Wendt A E 1995 *Appl. Phys. Lett.* **67** 3099

[17] Tarasov I, Ostapenko S, Nakayashiki K and Rohatgi A 2004 *Appl. Phys. Lett.* **85** 4346